RSC Advances

PAPER

View Article Online
View Journal | View Issue

Cite this: *RSC Adv.*, 2024, **14**, 36451

Bioactive secondary metabolites from fungal endophytes, *Penicillium oxalicum* and *Phoma herbarum*, associated with *Morus nigra* and *Ficus sycomorus*: an *in silico* study†

Mohamed M. M. AbdelRazek, [a] Ahmed M. Elissawy, [bc] Nada M. Mostafa, [b] Ashaimaa Y. Moussa, [b] Mohamed A. Elshanawany[a] and Abdel Nasser B. Singab *[bc]

Two pure fungal strains were isolated and identified from *Ficus sycomorus* and *Morus nigra*, namely, *Penicillium oxalicum* (OR673586) and *Phoma herbarum* (OR673589), respectively. The extract and fractions of secondary metabolites of each fungus were evaluated for antioxidant, anti-inflammatory, antimicrobial, antibiofilm, antidiabetic, and cytotoxic activities. The chloroform fraction of *P. oxalicum* showed potent cytotoxic activity (IC_{50} = 7.695 μg mL^{-1}) against Hep-G2 cell line, alongside moderate antioxidant and anti-inflammatory activities. On the other hand, the *P. herbarum* chloroform fraction showed potent antioxidant (DPPH IC_{50} = 5.649 μg mL^{-1}) and antidiabetic activities (IC_{50} = 14.91 μg mL^{-1}) against inhibition of α-glucosidase, in addition to moderate cytotoxicity, anti-inflammatory, and antimicrobial activities. Guided cytotoxic fractionation leads to identifying bioactive compounds using hyphenated techniques. LC-MS identified fourteen compounds for *P. herbarum* and thirteen compounds for *P. oxalicum*. Three known compounds, mevalolactone (**1**), glycerol monolinoleate (**3**), and ergosterol (**7**) in addition to one new compound, barcelonyl acetate (**2**), were isolated from *P. herbarum*. On the other hand, four known compounds, 4-hydroxyphenyl acetic acid (**4**), secalonic acid D (**5**), altersolanol A (**6**), and ergosterol (**7**), were isolated from *P. oxalicum*. Altersolanol A (**6**) and secalonic acid D (**7**) exhibited outstanding cytotoxic activity against Hep-G2 and Caco-2 cell lines, with IC_{50} values ranging from 0.00038 to 0.208 μM. *In silico* study findings showed altersolanol A (**6**), 4-hydroxyphenyl acetic acid (**4**), glycerol monolinoleate (**3**), and barcelonyl acetate (**2**) displayed significant potential but may benefit from further optimization as lead for developing potent c-Jun N-terminal kinase 2 (JNK2, PDB: 3NPC) inhibitors, potentially leading to novel therapeutic strategies targeting cancer therapy.

Received 22nd September 2024
Accepted 31st October 2024

DOI: 10.1039/d4ra06840h

rsc.li/rsc-advances

1. Introduction

Ficus sycomorus and *Morus nigra* are medicinal plants used traditionally to treat different diseases in many parts of Africa and Asia.[1,2] Endophytic fungi proved a promising source for optimizing new resources in drug discovery. Endophytic fungi contain a wealth of chemical classes, such as polyketides, alkaloids, coumarins, xanthones, anthraquinones, phenols, phenolic acids, terpenoids, steroids, sterols, and miscellaneous compounds.[3–5] These are promising metabolites for developing potential medication candidates with bioactivities such as cytotoxic, antibiofilm, antiviral, anti-inflammatory, anthelmintic, antidiabetic, antioxidant, antibacterial, antifungal, and immune-modulating activities.[6,7]

Through the last two decades, many reports have described the endophytic fungi associated with medicinal plants belonging to the family Moraceae. Many endophytic fungi isolates were reported from *Morus alba* from various tissues (leaves, stems, and roots), with *Fusarium* being the most prevalent genus. Among these isolates, a majority were successfully identified as genera *Alternaria*, *Phoma*, *Colletotrichum*, *Aspergillus*, *Macrophomina*, *Penicillium*, and *Scytalidium*, while the remaining isolates were classified as undefined.[8–14] However, one endophytic fungal strain was reported of *Morus* plants as *Botryosphaeria* sp. for *M. nigra*, *Phomopsis* sp. for *M. cathayana*, and seven undefined strains for *M. macroura*.[15–17]

A limited number of articles reported the biological activities of endophytic fungal extracts associated with *Morus* plants evaluated for antifungal, antioxidant, antiviral, antidiabetic, and antibiofilm potential. In addition, few articles reported the

[a]*Department of Pharmacognosy, Faculty of Pharmacy, Badr University in Cairo (BUC), Cairo 11829, Egypt*

[b]*Department of Pharmacognosy, Faculty of Pharmacy, Ain-Shams University, Cairo 11566, Egypt. E-mail: vpr.nassersingab@asu.edu.eg*

[c]*Center of Drug Discovery Research and Development, Ain Shams University, Cairo 11566, Egypt*

† Electronic supplementary information (ESI) available: Fig. S1–S36 and Tables S1–S8. See DOI: https://doi.org/10.1039/d4ra06840h

isolation of compounds from endophytic fungi associated with *Morus* plants. The reported compounds belong to diverse chemical classes, including anthraquinones, quinones, pyrones, naphthoquinones, polyketides, oxazole derivatives, and furoic acid derivatives that were tested for various biological potentials of neuroprotective, antioxidant, antimicrobial, antimalarial, glucose inhibitory, hemolytic, and cytotoxic activities.[7,8,10,11,16,18]

However, *Ficus* endophytic fungal strains were reported of the genera *Penicillium* and *Aspergillus* as the most frequently identified endophytes. Few works reported the endophytic fungi associated with *Ficus* plants: *F. elastica*, *F. carica*, *F. microcarpa*, *F. hirta*, *F. religiosa*, and *F. sphenophyllum*.[19–27] The reported studies on *Ficus*-associated endophytes showed cytotoxic, antioxidant, antidiabetic, antibacterial, and antifungal potential of the fungal extracts associated with *F. elastica* and *F. religiosa*.[28,29] Endophytic fungi associated with *F. elastica*, *F. carica*, and *F. hirta* were reported to have different chemical classes of isolated compounds, including xanthones, alkaloids, chromones, isochromenones, cyclopentenones, polyketides, and triterpenoids. The activities of these compounds were evaluated for antioxidant, antibacterial, and antifungal to neuraminidase inhibitory and herbicidal potential.[19–28]

To our knowledge, the present study aims to characterize the endophytic fungi associated with *F. sycomorus* for the first time in addition to *M. nigra* of limited reported work. The study aims to evaluate the biological activities and chemical constituents of their active extracts and fractions as a potential source for further exploration of bioactive molecules for drug discovery and development. This study is part of an ongoing research project to investigate the active metabolites of endophytic fungi associated with Moraceae plants as an alternative eco-friendly source for active molecules.

2. Experimental section

2.1. Purification of the fungal endophytes

Morus nigra was collected from a farm in El-Monofia governorate, Egypt, while *Ficus sycomorus* was collected from El-Kanater Horticulture Research Station, El-Kalubia governorate, Egypt, in November 2020, identified by Prof. Abd El-Halim Abd El-Magly Mohamed (Horticulture Research Institute, Flora and Phytotaxonomy Research Unit, Egypt), and vouchered samples were kept at Ain Shams University under the codes PHG-P-MN-333 for *M. nigra* and PHG-P-FS-332 for *F. sycomorus*. The isolation and identification workup of the fungal strains were performed as previously reported.[30]

2.2. Cultivation, extraction, and isolation

Cultivation and fermentation of the fungal strains were performed as previously reported.[30] The crude extract yield of twelve 1 L flasks for each fungal strain was 35.614 g for *Penicillium oxalicum* and 35.614 g for *Phoma herbarum*. The crude extracts were partitioned between *n*-hexane and 90% aqueous methanol (MeOH). Then liquid/liquid fractionation was performed using a separating funnel multiple times with varying gradients, involving the following combinations: *n*-hexane: MeOH (90%), chloroform ($CHCl_3$): MeOH (60%), and ethyl acetate (EtOAc): MeOH (60%).[31,32] Three fractions were collected for each fungal strain. *P. herbarum* fractions yield 14.8211 g for the *n*-hexane fraction (PH1), 6.1490 g for the $CHCl_3$ fraction (PH2), 12.7969 g for the EtOAc fraction (PH3). While *P. oxalicum* yields 18.6911 g for the *n*-hexane fraction (PO1), 2.6845 g for the $CHCl_3$ fraction (PO2), 5.5356 g for the ethyl acetate fraction (PO3). Vacuum liquid chromatography (VLC) was applied for the fungal $CHCl_3$ fractions (PH2) and (PO2) on silica gel 60 eluting with gradient mobile phase (*n*-hexane-EtOAc 100 : 0 to 0 : 100, $CHCl_3$–MeOH 100 : 0 to 0 : 100) to give thirteen subfractions of each $CHCl_3$ fungal fraction. Various chromatographic techniques were employed to sequentially separate and refine the entire extract, such as VLC (Vacuum Liquid Chromatography), normal pressure CC (Column Chromatography), and semi-preparative HPLC (High-Performance Liquid Chromatography). Pure compounds were isolated and successively identified using diverse spectroscopic techniques.

2.3. Antioxidant evaluation

Antioxidant activity using the DPPH assay was evaluated as defined by.[33,34] The FRAP assay was performed as defined by.[35] Tested samples in the FRAP assay were of 1 mg mL^{-1} concentration. A calibration curve of Trolox was used, and results were expressed in μM Trolox equivalent per mL by substitution in the linear regression equation of the Trolox calibration curve ($Y = 0.0018X - 0.0340$, $R^2 = 0.9982$).

2.4. Cytotoxic evaluation

Cytotoxic activity was evaluated from the crude extracts and their fractions using the SRB assay as defined by,[36,37] against the liver cancer (Hep-G2) cell line, while the isolated fungal metabolites were tested against colon cancer (Caco-2) and liver cancer (Hep-G2) cell lines, and doxorubicin was used as a positive control. Crude extracts and their fractions were prepared in methanol of serial concentrations 1000, 100, 10, 0.1, and 0.01 μg mL^{-1}, while for isolated fungal metabolites of serial concentrations 1000, 100, 10, 0.1, 0.01, and 0.001 μg mL^{-1}. Absorbance was measured at 540 nm using a microplate reader (BMG Labtech-FLUO star Omega, Ortenberg, Germany).

2.5. Anti-inflammatory evaluation

The anti-inflammatory activity was performed by measuring the nitric oxide inhibitory activity of murine macrophage RAW264.7 cells using the assay as defined.[38,39] L-NAME was used as a positive control. The nitric oxide (NO) inhibitory activity was measured at 540 nm using a microplate reader (BMG Labtech-FLUO star Omega, Ortenberg, Germany).

2.6. Antimicrobial evaluation

The agar well diffusion method was performed to evaluate the antimicrobial activity as defined by.[40] Samples were prepared for the agar well diffusion assay of 20 mg mL^{-1} concentration. While the minimum inhibitory concentration was done using

a microtiter plate turbidity assay as defined by[41–43] against three microorganisms: *Staphylococcus aureus* (ATCC-6538), *Pseudomonas aeruginosa* (ATCC-9027), and *Candida albicans* (ATCC-10231). Gentamicin (MEMPHIS, Egypt) was used as positive control.

2.7. Antibiofilm inhibitory assay

The biofilm inhibitory activity was performed against *Pseudomonas aeruginosa* (ATCC-9027) using the assay as defined by.[44] Samples were dissolved in 10% DMSO and prepared in serial concentrations of 10, 5, 2.5, 1.25, and 0.625 mg mL^{-1}. The reaction mixture was read spectrophotometrically after gently shaking on a microplate reader (BioTek 800 TS, Agilent, USA) at 630 nm wavelength.

2.8. Antidiabetic evaluation

The antidiabetic activity was tested using α-glucosidase inhibitory assay as defined by.[45,46] Acarbose was used as a positive control. Samples were dissolved in DMSO, and serial dilutions were prepared. The enzymatic activity was measured at 405 nm using a microplate reader (BMG Labtech-FLUO star Omega, Ortenberg, Germany).

2.9. Liquid chromatography-mass spectrometry (LC-MS)

The LC-MS experiments were conducted using a triple quadruple instrument, C-18 column: 1.7 μm, particle size 2.1 × 50 mm (XEVO TQD, Waters Corporation, Milford, USA) located at the Center for Drug Discovery, Research, and Development, Faculty of Pharmacy, Ain Shams University.[47,48]

2.10. Nuclear magnetic resonance (NMR) spectroscopy

The NMR experiments were conducted using a Bruker Ascend 400/R spectrophotometer (Bruker®, AVANCE III HD, 400 MHz, Switzerland) located at the Center for Drug Discovery, Research and Development, Faculty of Pharmacy, Ain Shams University.[44]

2.11. Protein and ligand preparation

The library of natural compounds was downloaded from the purchasable "natural products" library from the Zinc server,[49] a freely accessible web-based server. The LigPrep module of Maestro was used to prepare the ligands at the standard setting and under the OPLS4 forcefield. The crystal structure of JNK2 complexed with the co-crystal BIRB796 was obtained from the protein data bank (PDB: 3NPC, 2.35 angstrom (Å)).[50] The protein was prepared by removing water molecules and the AZD3229 analog, along with the addition of any missing residues and hydrogen atoms. Following that, the prepared protein structure was protonated at physiological pH. Finally, the energy was minimized by employing a conjugate gradient method based on the OPLS-2005 force field, which produced a unique low-energy minimum of the structure.[51]

2.12. Molecular docking

A molecular docking study was carried out from the hits identified in the virtual screening and fragment-based studies. To avoid false positives, each ligand was docked in the binding site using Glide's extra precision module, yielding 32 poses for each ligand. The 2D interaction diagrams were generated employing the BIOVIA Discovery Studio Visualizer 2022 package, and the docking scores were ranked, with the most negative scores chosen for each complex. Docking validation was carried out by redocking the BIRB796 analog (co-crystal) and calculating the RMSD value (root-mean-square deviation).

3. Results and discussion

3.1. Morphological identification of *M. nigra* and *F. sycomorus* -associated endophytes

Two endophytic fungi were isolated from plants of the family Moraceae. The first strain encoded MN14 was isolated from the stem tissue of *Morus nigra* and exhibited distinctive characteristics, including ellipsoidal-shaped conidia measuring 4 × 3.5 μm, swollen phialides with a diameter of 23.5 μm and a length of 4.5 μm, and swollen metulae measuring 12.0 μm in diameter and 3.8 μm in length. These microscopic features and the observation of conidiophores reaching a diameter of 4.5 μm confirmed the strain's classification as *Phoma* sp. (Fig. S1, see ESI†). The second strain encoded FS12 was isolated from the stem tissue of *Ficus sycomorus* and displayed characteristic features, including bi-verticillate hyphae resembling *Penicillium*. Microscopic examination revealed ellipsoidal-shaped conidia measuring 4 × 3.5 μm in breadth. The presence of swollen phialides and metulae, measuring 23.5 × 4.5 μm and 12.0 × 3.8 μm in diameter, respectively. Conidiophores were observed to reach a diameter of 4.5 μm. Further supporting its classification as *Penicillium* sp. (Fig. S2, see ESI†).

3.2. Molecular identification of *M. nigra* and *F. sycomorus* -associated endophytes

Phoma sp. MN14 fungal isolate from *Morus nigra* stem tissue and the *Penicillium* sp. FS12 fungal isolates from *Ficus sycomorus* stem tissue were sequenced using the genetic regions of the 18 s rRNA gene. When compared to similar sequences in the National Center for Biotechnology Information (NCBI) database, the *Phoma* isolate showed a 100% identity and 100% query coverage with *P. herbarum* BZYB, while the *Penicillium* isolates exhibited a 100% identity and 100% query coverage with *P. oxalicum* SL2. Alignment analysis using MEGA10 software revealed no differences in the 1653 base pairs analyzed for the *Phoma* isolate and 1649 for the *Penicillium* isolate. The evolutionary relationships of taxa were examined through Neighbour-Joining tree analysis and phylogenetic tree bootstrap analysis, confirming the alignment results (Fig. S3 and S4, see ESI†). The sequences of *P. herbarum* MN14 isolate and *P. oxalicum* FS12 isolate were deposited in GenBank under the accession numbers OR673589 and OR673586, respectively.

3.3. Antioxidant activity

P. herbarum $CHCl_3$ fraction (PH2) showed potent antioxidant activity with DPPH IC_{50} values of 5.649 ± 0.47 μg mL^{-1}

compared to Trolox as a positive control with IC_{50} value of 7.217 ± 0.309 μg mL^{-1}. The result was confirmed by the FRAP assay that showed value of 2926.48 ± 142.654 μM Trolox equivalent per mL. *P. herbarum* total extract (PHT) and its ethyl acetate fraction (PH3) in addition to *P. oxalicum* $CHCl_3$ fraction (PO2) showed moderate antioxidant activity with IC_{50} values ranging from 38.95 ± 1.79 to 198 ± 7.76 μg mL^{-1}. However, *P. herbarium* *n*-hexane fraction (PH1) in addition to *P. oxalicum* total extract (POT) and its *n*-hexane fraction (PO1) showed weak antioxidant activity with DPPH IC_{50} greater than 200 μg mL^{-1} (Table S1, see ESI†).

3.4. Cytotoxic activity

The total extracts and their fractions were tested for cytotoxic activity. The most potent cytotoxic activity against liver cancer (Hep-G2) cell line was *P. oxalicum* $CHCl_3$ fraction (PO2) with IC_{50}value of 7.695 μg mL^{-1}, followed by moderate activity of *P. herbarum* $CHCl_3$ fraction (PH2) that showed an IC_{50} value of 77.8 μg mL^{-1}. *P. oxalicum* and *P. herbarum* total extracts and their other fractions showed weak cytotoxic activity with IC_{50} values greater than 100 μg mL^{-1} against Hep-G2 compared to doxorubicin as a positive control with IC_{50} value of 0.87 μg mL^{-1} (Table S2, see ESI†).

The isolated compounds were tested against colon cancer cell line (Caco-2), and liver cancer (Hep-G2), while doxorubicin was used as a control drug as shown in Table 1. Altersolanol A (**6**) from *P. oxalicum* (*PO*) showed potent cytotoxic activity with IC_{50} values of 0.00038 ± 0.0003 μM against Hep-G2, and 0.044 ± 0.004 μM against Caco-2. Secalonic acid D (**5**), also isolated from *PO*, displayed a potent cytotoxic activity with IC_{50} values of 0.032 ± 0.0003 μM against Hep-G2, and 0.007 ± 0.001 μM against Caco-2. Another compound from *PO*, 4-hydroxyphenyl acetic acid (**4**), showed a moderate cytotoxic activity with IC_{50} values of 15.51 ± 2.03 μM against Hep-G2 cells, and 38.27 ± 2.20 μM against Caco-2. On the other hand, *P. herbarum* (*PH*) isolated compound, mevalonolactone (**1**) showed weak cytotoxic activity with IC_{50} values of 919.47 ± 79.76 μM against Hep-G2, and 872.14 ± 126.71 μM against Caco-2 cells. Barcelonyl acetate (**2**) isolated from *PH* showed moderate cytotoxic activity with IC_{50} values of 163.44 ± 12.23 μM against Hep-G2, and 110.90 ± 7.37 μM against Caco-2. Additionally, glycerol monolinoleate (**3**) from *PH* showed moderate cytotoxic activity with IC_{50} values of 166.53 ± 18.23 μM against Hep-G2, and 70.63 ± 8.50 μM against Caco-2. The results were compared with the control drug, doxorubicin, on the same cell lines that exhibited IC_{50} values of 0.2226 ± 0.06 μM against Hep-G2, and 0.401 ± 0.02 μM against Caco-2. These findings provide significant insights into the potential anti-cancer activity of the isolated compounds, highlighting their varying effectiveness against different cell lines.

Table 1 Cytotoxic activity of the isolated fungal metabolites against different cell lines[a]

SN	Isolated compound	IC_{50} (μM)	
		Hep-G2	Caco-2
1	Mevalonolactone	919.47 ± 79.76	872.14 ± 126.71
2	Barcelonyl acetate	163.44 ± 12.23	110.90 ± 7.37
3	Glycerol monolinoleate	166.53 ± 18.23	70.63 ± 8.50
4	4-Hydroxyphenyl acetic acid	15.51 ± 2.03	38.27 ± 2.20
5	Secalonic acid D	**0.032 ± 0.0003**	**0.007 ± 0.001**
6	Altersolanol A	**0.00038 ± 0.0003**	**0.044 ± 0.004**
—	Dox	**0.2226 ± 0.06**	**0.401 ± 0.02**

[a] Hep-G2: Liver Cancer Cell line, Caco-2: Colon Cancer Cell line, Dox.: Doxorubicin was used as a positive control drug.

3.5. Anti-inflammatory activity

P. herbarium $CHCl_3$ fraction (PH2), *n*-hexane fraction (PH1), and *P. oxalicum* $CHCl_3$ fraction (PO2) showed potent nitric oxide inhibitory activity with IC_{50} values of 26.51, 17.82, and 14.68 μg mL^{-1}, respectively. *P. herbarum* EtOAc fraction (PH3), in addition to *P. oxalicum* *n*-hexane fraction (PO1), showed moderate activity with IC_{50} values of 76.09 and 65.99 μg mL^{-1}, respectively. However, *P. herbarum* total extract (PHT) in addition to *P. oxalicum* total extract (POT) showed weak nitric oxide inhibitory activity with IC_{50} values greater than 100 μg mL^{-1} compared to nitro-L-arginine methyl ester hydrochloride (L-NAME) as a positive control that showed IC_{50} value of 7.316 μg mL^{-1} (Table S3, see ESI†).

3.6. Antimicrobial activity screening

P. herbarum total extract (PHT) and its $CHCl_3$ fraction (PH2) showed antimicrobial activity using the agar well diffusion assay of the tested sample concentration of 20 mg mL^{-1} that showed inhibition zones ranging from 22 to 38 mm against the tested Gram-positive *Staphylococcus aureus* ATCC-6538, Gram-negative bacteria *Pseudomonas* aeruginosa ATCC-9027, and the tested fungal strain *Candida albicans* ATCC-10231. Moreover, the microtiter plate dilution assay was conducted to confirm the activity that displayed minimum inhibitory concentration (MIC) values ranging from 2 to 4 mg mL^{-1}. However, *P. herbarium* *n*-hexane fraction (PH1) showed weak antimicrobial activity with inhibition zones ranging from 12 to 15 mm against the tested organisms and MIC values ranging from 3 to 8 compared to the negative control. While *P. oxalicum* total extract and all its fractions showed selective moderate antimicrobial activity against Gram-positive *S. aureus* with inhibition zones ranging from 17 to 29 mm. However, they displayed weak activity against Gram-negative bacteria *P. aeruginosa* and the tested fungal strain *C. albicans*, with inhibition zones ranging from 10 to 21 mm of the agar well diffusion assay and MIC values ranging from 4 to 12 mg mL^{-1} of the microtiter plate dilution assay. Gentamicin was used as a positive control and showed inhibition zones ranging from 34 to 40 mg mL^{-1} in the agar well diffusion assay and MIC values of 0.003125 to 0.0125 mg mL^{-1} in the microtiter plate turbidity assay (Table S4, see ESI†).

3.7. Antibiofilm activity

P. herbarum *n*-hexane fraction (PH1) and $CHCl_3$ (PH2) fraction, in addition to *P. oxalicum* *n*-hexane fraction (PO1), showed antibiofilm inhibitory activity against *Pseudomonas aeruginosa* ATCC-9027 in a dose-dependent manner and showed minimum biofilm inhibitory concentration (MBIC) values of 1.25, 5, and

2.5 mg mL^{-1}. However, the total extracts of *P. herbarum* and *P. oxalicum* showed weak activity with MBIC values greater than 10 mg mL^{-1} (Table S4, see ESI†).

3.8. Antidiabetic activity

P. herbarium $CHCl_3$ fraction (PH2) showed α-glucosidase enzyme inhibitory activity in a dose-dependent manner and displayed IC_{50} values of 14.91 μg mL^{-1}. Followed by the moderate activity of *P. herbarum* total extract (PHT) and its EtOAc fraction (PO3) that showed IC_{50} of 79.17 and 148.5 μg mL^{-1}, respectively. *P. herbarum n*-hexane fraction in addition to *P. oxalicum* total extract (POT) and all its thereof fractions showed weak activity with IC_{50} values greater than 1000 μg mL^{-1} compared to acarbose as a positive control that showed IC_{50} value of 224.0 μg mL^{-1}. However, the $CHCl_3$ fraction (PO2) of *P. oxalicum* showed an inhibitory percentage of 46.16 ± 1.32% at the test's highest concentration of 1000 μg mL^{-1} (Table S5, see ESI†).

3.9. Chemical characterization of *P. herbarum* chloroform fraction (PH2) and *P. oxalicum* chloroform fraction (PO2)

P. herbarum $CHCl_3$ fraction (PH2) and chemical contestants were tentatively identified using LC/MS-positive-ESI analysis and compared with spectral data in the literature (Table S6 and Fig. S5, see ESI†). Thirteen compounds were identified as mevalonolactone (**1**), phomasparapyrone A, 8-hydroxy-pregaliellalactone B, phomactin B, tersone F, phomaether A, barcelonyl acetate (**2**), barceloneic acid C, terezine N, terezine L, alterporriol S, phomalide, glycerol monolinoleate (**3**), and ergosterol (**7**). The identified compounds exhibit a broad range of chemical structures, encompassing lactones, pyrone derivatives, polyketides, diterpenes, pyridine alkaloids, diphenyl ethers, terazine derivatives, pyrazine derivatives, anthraquinone derivatives, cyclic polypeptide derivatives, glycerides, and sterol. On the other hand, the investigation of the chemical constituents of *P. oxalicum* $CHCl_3$ fraction (PO2) showed thirteen identified compounds as mevalonolactone (**1**), 4-hydroxyphenyl acetic acid (**4**), 1,3-dihydroxypropan-2-yl 2,4-dihydroxy-6-methylbenzoate, 2-(4-hydroxybenzyl) quinazolin-4(3*H*)-one, penipanoid A, 2,5-dimethyl-7-hydroxychromone, coniochaetone J, meleagrin, meleagrin A; Me ether, penioxamide A, secalonic acid D (**5**), altersolanol A (**6**), and ergosterol (**7**). The compounds represented a wide range of structural classes including pyrone derivatives, phenolic acids, alkaloids, chromanone derivatives, xanthone derivatives, sterols, and anthraquinone derivatives (Table S7 and Fig. S5, see ESI†). This diversity suggests a wide

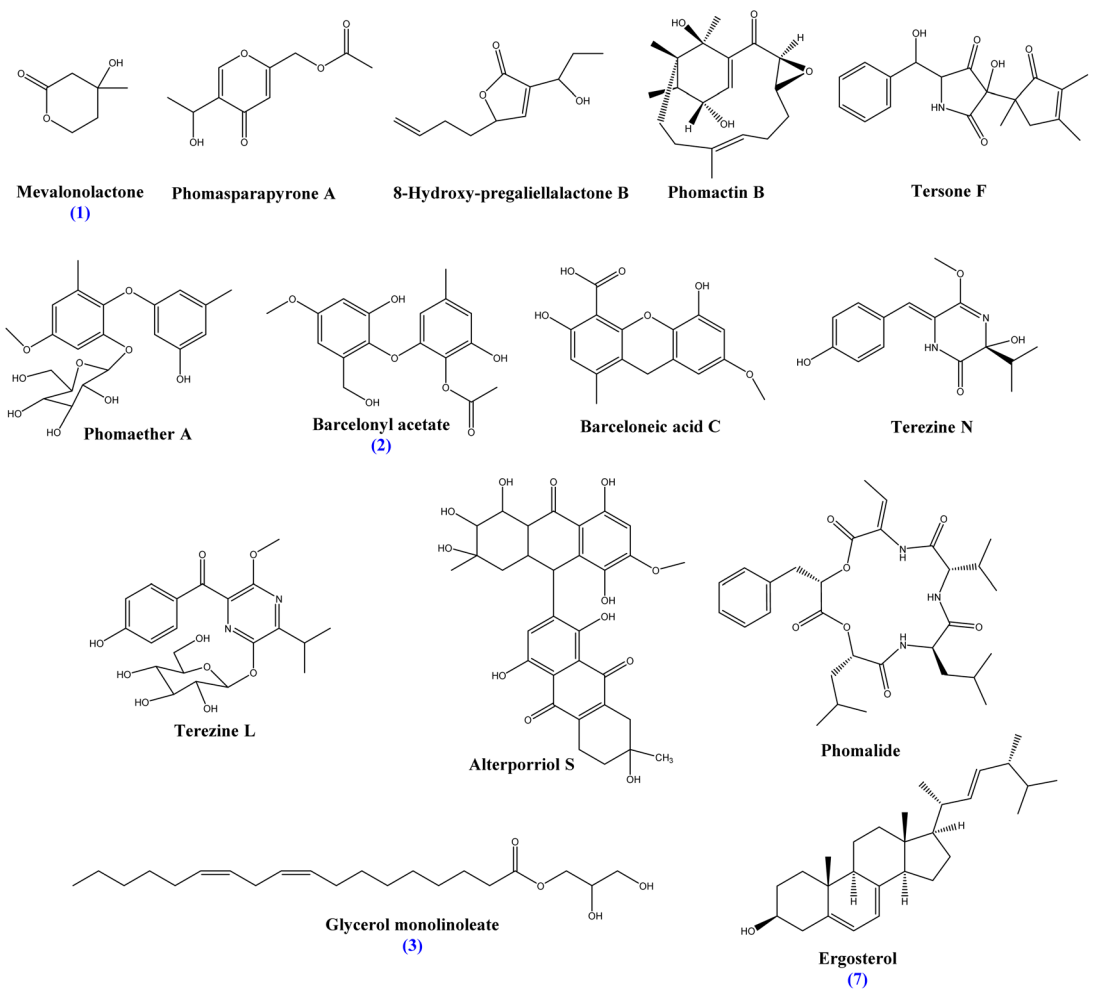

Fig. 1 Structure of the main identified constituents of *P. herbarum* chloroform fraction.

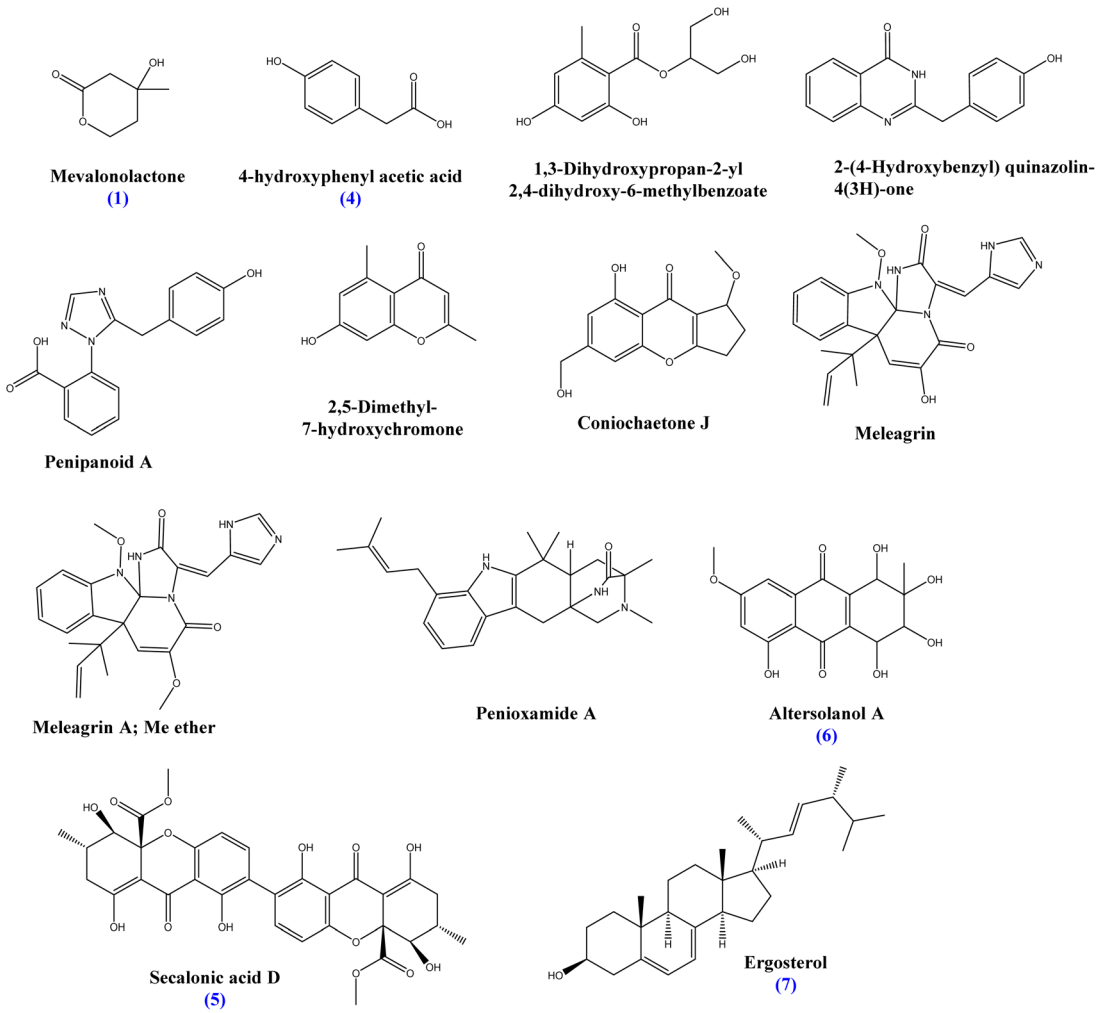

Fig. 2 Structure of the main identified constituents of *P. oxalicum* chloroform fraction.

array of biosynthetic pathways operating within these fungi. The structures of the major identified fungal metabolites are displayed in Fig. 1 and 2.

3.10. Identification of isolated compounds of fungal chloroform fractions

To explore the active metabolites present in the identified fungi, the total extracts were purified, isolating three known compounds: mevalolactone (**1**), glycerol monolinoleate (**3**), and ergosterol, in addition to one new barcelonic acid derivative namely barcelonyl acetate (**2**) from *P. herbarum* chloroform fraction, and four known compounds: 4-hydroxyphenyl acetic acid (**4**), secalonic acid D (**5**), altersolanol A (**6**), and ergosterol (**7**) from *P. oxalicum.* These compounds were identified based on their spectral NMR data, and a comparison was made with compounds previously reported in the literature.

Mevalonolactone (**1**): was separated as a yellow oil from *P. herbarum* chloroform fraction, yielding 14.5 mg of pale yellow oil, which was confirmed by reported NMR data[52,53] (ESI: Fig. S6–S9†). Mevalonolactone was previously reported from *Pestalotiopsis* sp. & *Penicillium solitum*.[54,55] This is the first time to isolate mevalonolactone from *P. herbarum* associated with *M. nigra*.

Barcelonyl acetate (**2**): was separated as a yellow oil from *P. herbarum* chloroform fraction, yielding 10 mg as yellowish oil, and was confirmed by the reported data of a closer structure, namely 8-*O*-methyl barceloneate, which are both derived from barceloneic acid A as described in Table 2.[56,57] The acetyl group was confirmed by the HMBC correlation of C-8 at $\delta_c = 170$ Hz with the 3H protons of carbon 9 at $\delta_H = 2.0$ Hz. The ^{1}HNMR, attached proton test (APT), and 2D NMR data confirmed the structure is a new compound, namely, 3-hydroxy-1-(2′-hydroxy-6′-(hydroxymethyl)-4′-methoxyphenoxy)-5-methylphenyl acetate, which is abbreviated to barcelonyl acetate (ESI: Fig. S10–S14†). This is the first time to report barcelonyl acetate from *P. herbarum* associated with *M. nigra*. Moreover, this is the first time to report this compound from nature (Fig. 3).

Glycerol monolinoleate (**3**): was separated as a colorless oil from *P. herbarum* chloroform fraction of yield 45.9 mg, which was confirmed by reported NMR data[58] (ESI: Fig. S15–S19†).

4-Hydroxyphenyl acetic acid (**4**): was separated as a white crystalline powder of *P. oxalicum* chloroform fraction of yield

Table 2 ^{1}H-NMR and APT assignment of barcelonyl acetate (2) compared to reported compound 8-*O*-methyl barceloneate

	Barcelonyl acetate (2)		8-*O*-Methyl barceloneate[56]	
Position	δ_C ($CDCl_3$, 100 MHz)	δ_H ($CDCl_3$, 400 MHz, J in Hz)	δ_C (125 MHz, $CDCl_3$)	δ_H (500 MHz, $CDCl_3$)
1	158.62	—	158.1	—
2	99.43	—	100.9	—
3	163.96	—	162.8	—
4	113.62	6.65 (d, J = 4.5, 1H)	112.6	6.51, d, (1.5)
5	147.60	—	147.2	—
6	104.60	5.94 (d, J = 7.1, 1H)	105.8	5.94, d, (1.5)
7	22.19	2.21, (s, 3H)	22.1	2.17, s
8	170.45	—	170.2	—
9	55.73	2.0, (s, 3H)	52.8	3.99, s
1′	130.36	—	132.7	—
2′	149.59	—	149.3	—
3′	103.37	6.57 (d, J = 11.0, 1H)	101.8	6.57, d, (3.0)
4′	157.31	—	157.9	—
5′	107.91	6.57 (d, J = 11.0, 1H)	105.8	6.59, d, (3.0)
6′	131.76	—	135.0	—
7′	61.61	4.94 (s, 2H)	61.0	4.50, s
8′	55.73	3.84 (s, 3H)	55.6	3.82, s

39.7 mg, which was confirmed by reported NMR data on 4-hydroxyphenyl acetic acid[59] (ESI: Fig. S20–S24†).

Secalonic acid D (**5**): it was separated as yellow gum of *P. oxalicum* chloroform fraction of yield 24.8 mg, which was confirmed by reported NMR data on secalonic acid D[60] (ESI: Fig. S25–S29†).

Altersolanol A (**6**): it was separated as orange crystals of *P. oxalicum* chloroform fraction of yield 8 mg, which was confirmed by reported NMR data[61] (ESI: Fig. S30–S34†). This compound was previously reported from *Stemphylium globuliferum*.[61,62] However, to our knowledge, it is the first time to report altersolanol A from *P. oxalicum*.

Ergosterol (7): was separated as colorless crystals from both *P. herbarum* and *P. oxalicum* chloroform fractions of yield 83.6 mg and 15.2 mg, respectively, which was confirmed by reported NMR data on ergosterol (ESI: Fig. S35–S36†).[63,64]

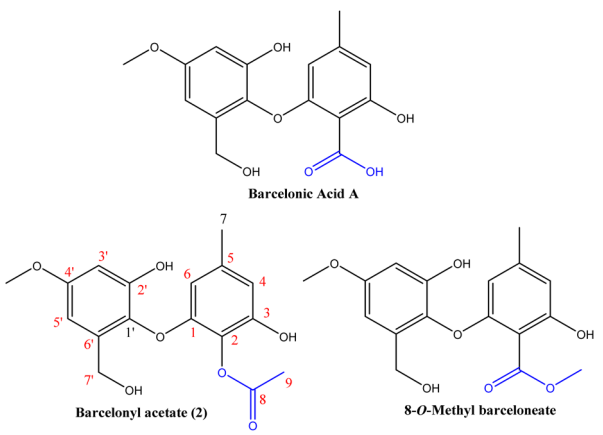

Fig. 3 Structure of the new isolated compound barcelonyl acetate (2) compared to closer molecules barceloneic acid A and 8-*O*-methyl barceloneate.

3.11. Molecular docking

JNK2 plays a multifaceted role in both cancer and inflammation. In some cancers, JNK2 acts as a tumor suppressor, promoting cell death and hindering the spread of cancer cells. However, in other cancers, JNK2 can encourage tumor growth. This complex relationship highlights the need for further research to understand the specific context in which JNK2 functions in different cancers. Similarly, JNK2 can be both anti-inflammatory and pro-inflammatory depending on the tissue and cell type. It can help maintain gut health and reduce inflammation, but also contribute to inflammatory processes in immune cells. Due to this complex interplay, targeting JNK2 with inhibitors holds promise for cancer and inflammatory disease treatment. If researchers can develop inhibitors that specifically target JNK2's pro-cancerous or pro-inflammatory functions, it could lead to novel therapeutic strategies. However, the challenge lies in creating inhibitors that are specific and don't disrupt JNK2's potentially beneficial functions in other contexts.

This molecular docking investigation studied the potential of several naturally isolated compounds as inhibitors of c-Jun N-terminal kinase 2 (JNK2) using a docking approach. The co-crystal inhibitor, BIRB796, served as a reference for evaluating the interaction patterns with JNK2. Identifying compounds that mimic BIRB796's interactions is crucial for discovering potent JNK2 inhibitors. BIRB796 forms a well-defined interaction profile with JNK2, including hydrogen bonds with key residues Met111, Glu73, and Asp169. It also engages in extensive pi–pi interactions with aromatic amino acids like Val40, Ala53, and Phe170, and a pi–sulfur interaction with Met108. These interactions provide a benchmark for assessing the binding potential of the natural compounds.

Among the evaluated compounds, 4-hydroxyphenyl acetic acid (**4**) displayed common interactions with BIRB796. It forms a hydrophobic interaction with Val40 and Lys55, suggesting

Table 3 The molecular docking scores and interactions of isolated compounds

Compound	Docking score	Interaction type	Interacting residues
Co crystal (BIRB796)	−9.687	Hydrogen bond	Met111, Glu73, Asp169
		Pi–pi	Val40, Ala53, Lys55, Arg69, Leu77, Ile85, Leu110, Leu142, Ile147, His149, Val158, Phe170
		Pi–sulfur	Met108
Mevalonolactone (**1**)	−5.998	Hydrogen bond	Asp169, Lys55
		Pi–pi	Leu168, Ile86
Barcelonyl acetate (**2**)	−6.769	Pi–anion	Asp169, Arg72
		Pi–alkyl	Arg150
		Pi–pi	Ala173, Gln37, Gly171, Arg69, Arg192, Asp151, His149, Ile147, Ile148, Leu76
Glycerol monolinoleate (**3**)	−6.719	Hydrogen bond	Met111
		Pi–pi	Val40, Leu77, Lys55, Ile85, Ile86, Val80, Leu168, Phe170
4-Hydroxyphenyl acetic acid (**4**)	−5.919	Pi–alkyl	Lys55, Leu168, Val40, Met108
Altersolanol A (**6**)	−7.094	Hydrogen bond	Asp169, Glu73, Lys55, Gly171, Gln73, Arg69
		Pi–pi	Ile85, Leu77, Ile86

favourable binding affinity. Additionally, altersolanol A (**6**) presented a compelling profile with hydrogen bonds matching BIRB796 and additional interactions with Lys55 and Gly171, potentially enhancing binding. These findings highlight altersolanol A (**6**) as a promising candidate for further development as JNK2 inhibitors. Secalonic aid D (**5**) failed in the docking as it couldn't fit the pocket of the receptor for molecular docking as it is a large molecule of molecular weight 638. Meanwhile, mevalonolactone (**1**) exhibited fewer interactions compared to other compounds. While it formed hydrogen bonds with Asp169 and Lys55, it lacked extensive pi–pi interactions, suggesting a need for optimization to improve its binding affinity and efficacy as a JNK2 inhibitor. Barcelonyl acetate (**2**) displayed robust interaction capabilities, mimicking BIRB796's pi–anion bonds with Asp169, and Arg72. It also shared key pi–alkyl interactions with Arg150 and pi–pi interactions, suggesting a strong binding potential similar to BIRB796. These findings warrant further investigation and development of barcelonyl acetate (**2**) as a JNK2 inhibitor. Meanwhile, glycerol monolinoleate (**3**) presented the most comprehensive interaction profile. It formed a hydrogen bond with Met111 and engaged in multiple pi–pi interactions with residues crucial for BIRB796 binding. This extensive overlap suggests a high binding affinity and strong potential for JNK2 inhibition. The molecular docking interactions of the investigated compounds are outlined in Table 3. The 2D and 3D interaction figures are provided in (ESI Table S8†).

4. Conclusions

The study reports for the first time the isolation and identification of two fungal endophytes, *Phoma herbarum* and *Penicillium oxalicum*, from *Morus nigra* and *Ficus sycomorus*, respectively. Biological evaluation of the fungal extracts and fractions revealed a range of activities, with the chloroform fractions generally exhibiting the most potent effects. *P. herbarum* chloroform fraction demonstrated potent antioxidant and antidiabetic potential. While *P. oxalicum* chloroform fraction showed potent cytotoxic activity.

Through bioactivity-guided isolation, seven compounds were obtained and identified from the active chloroform fractions. Barcelonyl acetate (**2**) was reported for the first time from nature from *P. herbarum* that showed moderate cytotoxic activity. In addition, altersolanol A (**6**) and secalonic acid D (**5**) from *P. oxalicum* exhibited the strongest cytotoxicity against various cancer cell lines. Molecular docking identified glycerol monolinoleate as a promising JNK2 inhibitor, while altersolanol A (**6**) and barcelonyl acetate (**3**) also showed favourable interaction profiles. Key residues involved in hydrogen bonding and pi–pi interactions with the compounds were determined. The bioactive potential demonstrated by *P. herbarum* and *P. oxalicum* extracts and fractions, as well as the isolated compounds, warrants further investigation of their mechanisms and therapeutic applications. The *in silico* findings provide valuable leads for developing novel JNK2 inhibitors. Future work will optimize derived hits for the discovery of bioactive natural products.

Data availability

All data generated or analyzed during this study are included in this published article (and its additional ESI file†).

Author contributions

Conceptualization, ANBS and MAE; methodology, MMM; validation, ANBS, MME, NMM, AYM, and AME; formal analysis, ANBS, AME; investigation, MMA and AME; resources, MMA and AME; data curation, MMA and AME; writing – original draft preparation, MMA; writing – review and editing, MMA, AME, and ANBS; visualization, ANBS and AME; supervision, ANBS, MAE, NMM, AYM, and AME; project administration, ANBS. All authors have read and agreed to the published version of the manuscript.

Conflicts of interest

The authors declare that they have no conflicts of interests.

Acknowledgements

Abdel Nasser Singab is thankful to Egyptian Science and Technology Development Funds (STDF) for their financial support through grant No. 46667 entitled "Sustainability of Lab. Capacities of the Center of Drug Discovery Research and Development."

Notes and references

1 M. A. Hossain, *J. King Saud Univ.*, 2019, **31**, 961–965.
2 S. H. Lim and C.-I. Choi, *Nutrients*, 2019, **11**, 437.
3 L.-W. Wang, Y.-L. Zhang, F.-C. Lin, Y.-Z. Hu and C.-L. Zhang, *Mini Rev. Med. Chem.*, 2011, **11**, 1056–1074.
4 S. S. El-hawary, A. S. Moawad, H. S. Bahr, U. R. Abdelmohsen and R. Mohammed, *RSC Adv.*, 2020, **10**, 22058–22079.
5 J. F. Imhoff, *Mar. Drugs*, 2016, **14**, 19.
6 A. N. B. Singab, N. M. Mostafa, Y. A. Elkhawas, E. Al-Sayed, M. M. Bishr, A. M. Elissawy, M. S. Elnaggar, I. M. Fawzy, O. M. Salama and Y.-H. Tsai, *Mar. Drugs*, 2022, **20**, 331.
7 M. M. M. AbdelRazek, A. M. Elissawy, N. M. Mostafa, A. Y. Moussa, M. A. Elanany, M. A. Elshanawany and A. N. B. Singab, *Molecules*, 2023, **28**, 1718.
8 J. H. Song, C. Lee, D. Lee, S. Kim, S. Bang, M.-S. Shin, J. Lee, K. S. Kang and S. H. Shim, *J. Nat. Prod.*, 2018, **81**, 1411–1416.
9 L. P. Zheng, Z. Zhang, L. Q. Xie, H. Y. Yuan and Y. Q. Zhang, *Adv. Mater. Res.*, 2013, **642**, 615–618.
10 S. Bang, H. Eun, J. Yun, D. Sik, S. Kim, S. Nam, D. Lee, K. Sung and S. Hee, *Bioorg. Chem.*, 2020, **105**, 104449.
11 H. G. Choi, J. H. Song, M. Park, S. Kim, C. Kim, K. S. Kang and S. H. Shim, *Biomolecules*, 2020, **10**, 91.
12 H. Ku, J. Baek, K. S. Kang and S. H. Shim, *Nat. Prod. Res.*, 2021, **0**, 1–7.
13 J. Vora, S. Velhal, S. Sinha, V. Patel and N. Shrivastava, *HIV Med.*, 2021, **22**, 690–704.
14 R. Ayesha and T. Iftikhar, *Pakistan J. Bot.*, 2010, **42**, 583–592.
15 A. Aparecida, J. C. Polonio, A. M. Bulla, D. Polli, J. C. Castro, L. C. Soares, V. A. De, V. Elisa, P. Vicentini, A. José, B. De Oliveira, J. E. Gonçalves, R. Aparecida, C. Gonçalves, J. Lúcio, B. A. De Abreu-filho, J. A. Pamphile, A. Aparecida, J. C. Polonio, A. M. Bulla, D. Polli, J. C. Castro, L. C. Soares, V. A. De Oliveira-junior, V. Elisa, P. Vicentini, A. José, B. De Oliveira and J. E. Gonçalves, *Nat. Prod. Res.*, 2021, **36**, 3158–3162.
16 E. Hermawati, L. D. Juliawaty and E. H. Hakim, *Rec. Nat. Prod.*, 2017, **11**, 315–317.
17 J. Lukša and E. Servienė, *J. Environ. Eng. Landsc. Manag.*, 2022, **28**, 183–191.
18 E. Hermawati, S. D. Ellita, L. D. Juliawaty, E. H. Hakim, Y. M. Syah and H. Ishikawa, *J. Nat. Med.*, 2021, **75**, 217–222.
19 A. S. Ratnayake, W. Y. Yoshida, S. L. Mooberry and T. K. Hemscheidt, *J. Org. Chem.*, 2001, **66**, 8717.
20 A. D. Allen, B. Cheng, M. H. Fenwick, B. Givehchi, H. Henry-riyad and A. Valerij, *J. Org. Chem.*, 2003, **68**, 1640.
21 E. V. Patridge, A. Darnell, K. Kucera, G. M. Phillips, H. R. Bokesch, K. R. Gustafson, D. J. Spakowicz, L. Zhou, W. M. Hungerford, M. Plummer, D. Hoyer, A. Narváez-Trujillo, A. J. Phillips and S. A. Strobel, *Nat. Prod. Commun.*, 2020, **10**, 1649–1654.
22 Z. Sun, F. Liang, Y. Chen, H. Liu and H. Li, *J. Asian Nat. Prod. Res.*, 2016, **6020**, 0–6.
23 Z. Sun, H. Li, F. Liang, Y. Chen, H. Liu and S. Li, *Molecules*, 2016, **21**, 1–6.
24 H. C. Zhang, Y. M. Ma, R. Liu and F. Zhou, *Biochem. Syst. Ecol.*, 2012, **45**, 31–33.
25 X. Liang, H. Zhang and R. Liu, *J. Agric. Food Chem.*, 2016, **64**, 7–11.
26 H. Zhang, Y. Ma and R. Liu, *Appl. Mech. Mater.*, 2012, **181**, 783–786.
27 X. A. Liang, Y. M. Ma, H. C. Zhang and R. Liu, *Nat. Prod. Res.*, 2016, **6419**, 2407–2412.
28 Z. Ding, T. Tao, L. Wang, Y. Zhao, H. Huang, D. Zhang, M. Liu, Z. Wang and J. Han, *J. Microbiol. Biotechnol.*, 2019, **29**, 731–738.
29 K. K. Jayant and B. S. Vijayakumar, *Ital. J. Mycol.*, 2021, **50**, 10–20.
30 A. Y. Moussa, N. M. Mostafa and A. N. B. Singab, *Nat. Prod. Res.*, 2019, **0**, 1–8.
31 S. M. Shama, A. M. Elissawy, M. A. Salem, F. S. Youssef, M. S. Elnaggar, H. R. El-Seedi, S. A. M. Khalifa, K. Briki, D. I. Hamdan and A. N. B. Singab, *RSC Adv.*, 2024, **14**, 18553–18566.
32 M. S. Elnaggar, A. M. Elissawy, F. S. Youssef, M. Kicsák, T. Kurtán, A. N. B. Singab and R. Kalscheuer, *RSC Adv.*, 2023, **13**, 16480–16487.
33 R. Boly, T. Lamkami, M. Lompo, J. Dubois and P. Guisson, *Int. J. Clin. Pharmacol. Res.*, 2016, **8**, 29–34.
34 Z. Chen, R. Bertin and G. Froldi, *Food Chem.*, 2013, **138**, 414–420.
35 D. N. Jamalova, H. A. Gad, D. K. Akramov, K. S. Tojibaev, N. M. Al Musayeib, M. L. Ashour and N. Z. Mamadalieva, *Plants*, 2021, **10**, 1529.
36 P. Skehan, R. Storeng, D. Scudiero, A. Monks, J. McMahon, D. Vistica, J. T. Warren, H. Bokesch, S. Kenney and M. R. Boyd, *JNCI, J. Natl. Cancer Inst.*, 1990, **82**, 1107–1112.
37 R. M. Allam, A. M. Al-Abd, A. Khedr, O. A. Sharaf, S. M. Nofal, A. E. Khalifa, H. A. Mosli and A. B. Abdel-Naim, *Toxicol. Lett.*, 2018, **291**, 77–85.
38 T. Oliveira, C. A. Figueiredo, C. Brito, A. Stavroullakis, A. Prakki, E. Da Silva Velozo and G. Nogueira-Filho, *Int. J. Cell Biol.*, 2014, **2014**, 535789.
39 M. S. Yoo, J. S. Shin, H. E. Choi, Y. W. Cho, M. H. Bang, N. I. Baek and K. T. Lee, *Food Chem.*, 2012, **135**, 967–975.
40 M. M. M. A. Razek, A. Y. Moussa, M. A. El-Shanawany and A. B. Singab, *Int. J. Pharm. Sci. Res.*, 2019, **11**, 3289–3296.
41 F. Barchiesi, J. Bille, E. Chryssanthou, D. Denning, J. P. Donnelly, B. Dupont, W. Fegeler, C. Moore, M. Richardson, P. E. Verweij, K. Hospital, N. Manchester,

G. Hospital and H. Hospital, *Clin. Microbiol. Infect.*, 2003, **9**, 1–8.
42 C. Rodr, C. Alonso-calleja, C. Garc, J. Carballo and R. Capita, *Biology*, 2022, **11**, 46.
43 R. Mogana, A. Adhikari, M. N. Tzar, R. Ramliza and C. Wiart, *BMC Complement. Med. Ther.*, 2020, **20**, 1–11.
44 M. M. M. AbdelRazek, A. Y. Moussa, M. A. El-shanawany and A. B. Singab, *Chem. Biodivers.*, 2020, **17**, 1–9.
45 R. Subramanian, M. Z. Asmawi and A. Sadikun, *Acta Biochim. Pol.*, 2008, **55**, 391–398.
46 H. M. Abdallah, A. T. Kashegari, A. A. Shalabi, K. M. Darwish, A. M. El-Halawany, M. M. Algandaby, S. R. M. Ibrahim, G. A. Mohamed, A. B. Abdel-Naim, A. E. Koshak, P. Proksch and S. S. Elhady, *Biology*, 2022, **11**, 762.
47 S. Saeed Kotb, I. M. Ayoub, S. A. El-Moghazy and A. N. B. Singab, *Nat. Prod. Res.*, 2022, 1–6.
48 S. H. Abdallah, N. M. Mostafa, M. A. E. H. Mohamed, A. S. Nada and A. N. B. Singab, *Nat. Prod. Res.*, 2022, **36**, 5619–5625.
49 J. J. Irwin and B. K. Shoichet, *J. Chem. Inf. Model.*, 2005, **45**, 177–182.
50 A. Kuglstatter, M. Ghate, S. Tsing, A. G. Villaseñor, D. Shaw, J. W. Barnett and M. F. Browner, *Bioorg. Med. Chem. Lett.*, 2010, **20**, 5217–5220.
51 H. Nada, S. Kim, S. Godesi, J. Lee and K. Lee, *J. Biomol. Struct. Dyn.*, 2023, **41**, 11904–11915.
52 M. Kishida, N. Yamauchi, K. Sawada, Y. Ohashi, T. Eguchi and K. Kakinuma, *J. Chem. Soc., Perkin Trans. 1*, 1997, 891–895.
53 Y. Ying, L. Zhang, W. Shan and Z.-J. Zhan, *Chem. Nat. Compd.*, 2014, **50**, 628–629.
54 Z. Xu, X. Wu, G. Li, Z. Feng and J. Xu, *Nat. Prod. Res.*, 2020, **34**, 1002–1007.
55 Z.-H. He, J. Wu, L. Xu, M.-Y. Hu, M.-M. Xie, Y.-J. Hao, S.-J. Li, Z.-Z. Shao and X.-W. Yang, *Mar. Drugs*, 2021, **19**, 580.
56 D. P. Overy, T. O. Larsen, P. W. Dalsgaard, K. Frydenvang, R. Phipps, M. H. G. Munro and C. Christophersen, *Mycol. Res.*, 2005, **109**, 1243–1249.
57 Y. Tan, Y. Wang, Q. Li, X. Xing, S. Niu, B. Sun, L. Chen, R. Pan and G. Ding, *Phytochemistry*, 2022, **201**, 113264.
58 E. Okuyama, T. H. Asegawa, T. M. Atsushita, H. F. Ujimoto and M. I. Shibashi, *Chem. Pharm. Bull.*, 2001, **49**, 154–160.
59 J. E. Milne, T. Storz, J. T. Colyer, O. R. Thiel, M. Dilmeghani Seran, R. D. Larsen and J. A. Murry, *J. Org. Chem.*, 2011, **76**, 9519–9524.
60 L. Chen, Y. X. Bi, Y. P. Li, X. X. Li, Q. Y. Liu, M. G. Ying, Q. H. Zheng, L. Du and Q. Q. Zhang, *Heterocycles*, 2017, **94**, 1766–1774.
61 A. Aly, A. Debbab, R. Edrada-Ebel, W. Muller, M. Kubbutat, V. Wray, R. Ebel and P. Proksch, *Mycosphere*, 2010, **1**, 153–162.
62 M. Teiten, F. Mack, A. Debbab, A. H. Aly, M. Dicato, P. Proksch and M. Diederich, *Bioorg. Med. Chem.*, 2013, **21**, 3850–3858.
63 A. Haque, M. S. Hossain, M. Z. Rahman, M. R. Rahman, S. Hossain, M. Mosihuzzaman, N. Nahar and S. I. Khan, *J. Pharm. Sci.*, 2005, **4**, 127–130.
64 R. X. Receptor, C. Xie, D. Zhang, J. Xia, C. Hu, T. Lin, Y. Lin, G. Wang, W. Tian, Z. Li, X. Zhang, X. Yang, H. Chen and M. Drugs, *Mar. Drugs*, 2019, **17**, 178.